## Electronic Supplementary Information (ESI)

# Hollow PtCo alloy nanostructures for efficient oxygen reduction electrocatalysis in polymer electrolyte membrane fuel cells

Muhammad Irfansyah Maulana,[a] Ha-Young Lee,[ab] Caleb Gyan-Barimah,[a] Jong Hun Sung [a] and Jong-Sung Yu *[ab]

[a] Department of Energy Science and Engineering, Daegu Gyeongbuk Institute of Science and Technology (DGIST), Daegu 42988, Republic of Korea. E-mail: jsyu@dgist.ac.kr

[b] UE Science, R7-507, 333 Techno Jungang-daero, Hyeonpung-eup, Dalseong-gun, Daegu 42988, Republic of Korea.

**Experimental**

*Chemicals*. Platinum(II) acetylacetonate (97%), cobalt(II) acetylacetonate (97%), oleylamine (technical grade, 70%), and oleic acid (technical grade, 90%) were purchased from Sigma Aldrich. Pt solution ($H_2PtCl_6 \cdot xH_2O$) was from Kojima Chemicals. Acetic acid (glacial, 95.0%), hexane (≥95.0%), and ethanol (≥99.8%) were purchased from Samchun. Commercial Pt/C (20 wt.% Pt loading) and commercial carbon (Ketjen Black EC300JD) were obtained from Tanaka and Ketjen Black International, respectively. All chemicals were used as received without any further purification treatment. Deionized water (Millipore, Milli-Q gradient) was used in all experiments.

*Synthesis of PtCo solid core-shell nanoparticles*. An appropriate amount of platinum(II) acetylacetonate and cobalt(II) acetylacetonate was added to the mixture of 8 mL oleylamine and 2 mL oleic acid in a three-neck flask equipped with a reflux system. The amount of Pt and Co precursors added to the solution was varied with the Pt/Co mol ratio of 1/2, 1/1, 2/1, and 3/1 to generate the solid core intermediates of $PtCo_2$-SC, $Pt_1Co_1$-SC, $Pt_2Co$-SC, and $Pt_3Co$-SC NPs, respectively. The precursor solution was then heated up to 180 °C under nitrogen purging and kept at that temperature for 2 h under vigorous stirring to generate the metal seed solution. To introduce the Pt shell, the specific amount of Pt precursor ($H_2PtCl_6 \cdot xH_2O$) solution was added just before the reaction temperature was increased to 240 °C. After 2 h stirring and heating at 240 °C under argon atmosphere, the reaction was rapidly cooled down by placing the flask in a water bath. The mixture of 10 mL hexane and 30 mL ethanol was added to the yielded solution at room temperature to initiate the precipitation of PtCo-SC@Pt NPs. The NPs were collected by centrifugation (7,000 rpm for 10 min) and washed three times with the mixture of hexane and ethanol.

*Evolution of PtCo solid core-shell to hollow core-shell nanoparticles*. An amount of PtCo-SC@Pt NPs was etched in 25 mL acetic acid at 70 °C for 12 h purging with oxygen gas. The final product was collected by centrifugation (14,000 rpm for 10 min) and washed three times with the mixture of hexane and ethanol. The etched PtCo-HC@Pt hollow core-shell catalysts were dried under vacuum at room temperature to finally produce PtCo-HC@Pt NPs. The above etching process was performed in the double-neck flask with a reflux system to ensure no loss of reactants.

*Catalyst loading*. The PtCo-HC@Pt NPs were dispersed in hexane. A specific amount of commercial carbon was subsequently added to the as-dispersed NPs to make a total metal (Pt+Co) loading in the range of ~20%, followed by stirring overnight to finish the loading process. The as-loaded NPs were

collected by centrifugation (14,000 rpm for 10 min) and washed three times with ethanol. The PtCo-HC@Pt/C catalysts were finally dried under vacuum at room temperature.

*Characterizations*. The crystalline nature of the samples was determined by X-ray diffraction (XRD) using Rigaku Smartlab diffractometer with Cu-Kα source (0.15406 nm) operated at 40 kV and 30 mA. The transmission electron microscope (TEM) images were acquired using FEI Tecnai G2 F20 to determine the size and morphology. The high-angle annual dark-field scanning transmission electron microscopy (HAADF-TEM) and quantitative energy dispersive spectroscopy (EDS) were carried out by FEI Themis Z to confirm the structure and characterize the elemental distribution. To analyze the surface behavior of the samples, X-ray photoelectron spectroscopy (XPS) measurement was conducted with AXIS-NOVA (Kratos) X-ray photoelectron spectrometer using a monochromated Al Kα X-ray source ($h\nu$ = 1486.6 eV) operated at 150 W. Thermogravimetric analysis (TGA) was performed using PerkinElmer Pyris instrument to confirm the total metal loading of the prepared catalysts. The chemical compositions of the samples were calculated by inductively coupled plasma optical emission spectroscopy (ICP-OES) using Thermo Scientific iCAP7400. The elemental analysis of the catalyst on the membrane was performed by micro-X-ray fluorescence spectroscopy (μ-XRF) using Horiba XGT-9000 Pro. The X-ray absorption spectroscopy (XAS) measurements were conducted at Pohang Accelerator Laboratory (PAL) and analyzed with the software of Demeter.

*Electrochemical half-cell test*. The half-cell test was carried out in which an electrochemical analyzer (Biologic VMP3) was connected to the RDE system. Prior to the electrochemical tests, the as-prepared PtCo-SC@Pt/C and PtCo-HC@Pt/C catalysts were annealed at 300 °C for 2 h in $H_2$/Ar to remove all the oxygenated species. The as-prepared catalyst or commercial Pt/C coated on a glass carbon electrode was used as the working, a calibrated Ag/AgCl saturated with KCl as the reference, and Pt wire as the counter electrodes. For the working electrode, the slurry was made by dispersing 2.5 mg of the catalyst powders in 0.49 mL solution consisting of 4 mL deionized water, 0.95 mL isopropanol, and 0.4 mL of 0.5 wt% Nafion solution, followed by ultra-high sonication until a uniform solution was observed. An amount of the slurry was drop-casted on the working electrode to achieve a Pt loading of 5 μg $cm^{-2}$. Prior to ORR linear sweep voltammetry (LSV) measurements, 30 cyclic voltammetry (CV) cycles were run under a scan rate of 50 mV $s^{-1}$ for activation. The measurements were conducted in both $N_2$- and $O_2$-saturated 0.1 M $HClO_4$ solution. The LSVs were obtained using a scan rate of 10 mV $s^{-1}$ at a rotating speed of 1600 rpm. All potentials were converted from Ag/AgCl to RHE using the equation $E_{RHE} = E_{Ag/AgCl} + 0.256$. The kinetic currents were obtained using Koutecky-Levich

equation, $j_k = j \times j_d/(j_d - j)$, where $j$ represents the experimentally measured current density and $j_k$ and $j_d$ are kinetic and diffusion-limited current densities.

*PEMFC single-cell test*. The performance of as-prepared catalyst and commercial Pt/C as cathode catalysts in a single cell system was investigated using a membrane electrode assembly (MEA) with an active area of 5 $cm^2$ manufactured using the catalyst coated membrane (CCM) method. For all the tests, commercial Pt/C was employed as an anode catalyst. To make the catalyst slurries, a mixture of catalyst powder, 2-propanol, and a 5 wt.% Nafion ionomer solution (Sigma Aldrich) was first ultrasonicated for 60 min. The slurries were directly sprayed onto a Nafion N211 membrane to make the catalyst layer, followed by drying at 60 °C for 12 h. Subsequently, the MEAs were fabricated using commercial gas diffusion layers (GDLs, SGL 39BB) without the use of hot-pressing. For both the anode and cathode, the catalyst loading was kept constant at 0.10 $mg_{metal}$ $cm^{-2}$. The prepared MEA cell was evaluated at using a PEMFC test station (Scitech Inc., KOREA) and an electronic load (PLZ664WA, Kikusui). The MEA polarization curves were recorded at 80 °C and relative humidity (RH) 100%. The back pressure of the anode and cathode sections was set at 150 $kPa_{abs}$. During measurements, fully humidified hydrogen (300 $cm^3$ $min^{-1}$) and fully humidified oxygen (1000 $cm^3$ $min^{-1}$) were flowed into the anode and cathode side, respectively. The current-voltage curves were recorded using constant current mode ascending from 0 A $cm^{-2}$ to limiting current density, evaluated in a step of 0.02 A $cm^{-2}$ with a holding time of 5 s for each point. For accelerated stress test (AST), according to electrocatalyst cycle protocols from the US Department of Energy (see Fig. S10), the MEA was wave-square cycled between 0.6 and 0.95 V with a hold-time of 3 sec at both potentials while feeding fully humidified hydrogen (100 $cm^3$ $min^{-1}$) and nitrogen (50 $cm^3$ $min^{-1}$) to anode and cathode, respectively, at 80 °C and ambient pressure. For mass activity measurements, the $H_2$–$O_2$ cell was operated at 80 °C, 150 $kPa_{abs}$ back pressure, RH 100 %, 2/9.5 anode/cathode stoichiometry, held at 0.9 V for 15 min to get multiple points, with the Pt mass activity recorded by averaging the last-minute value.

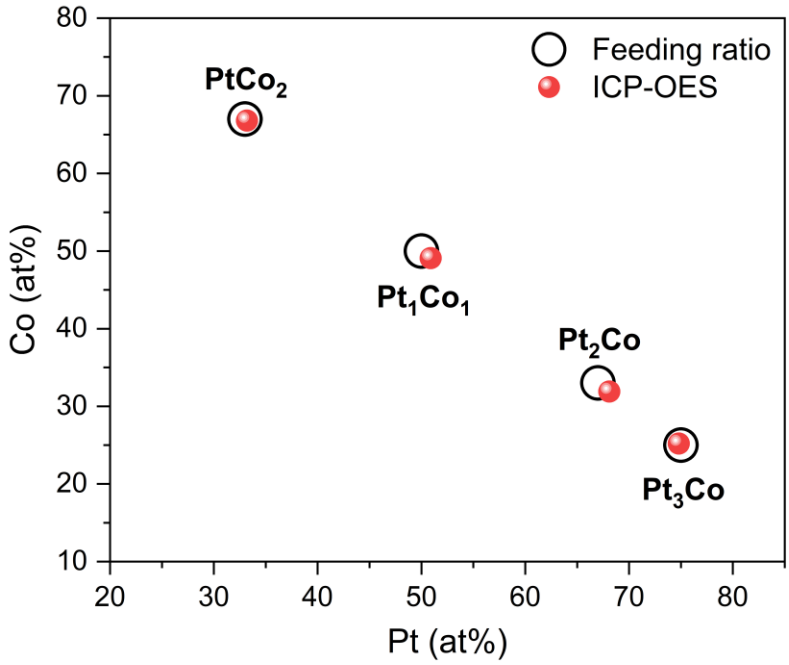


**Fig. S1.** Plot showing the design of Pt–Co in forms of Pt and Co atomic percentages determined by ICP-OES (red dot circle) and the actual feeding ratios of alloy compositions (black hollow circle).

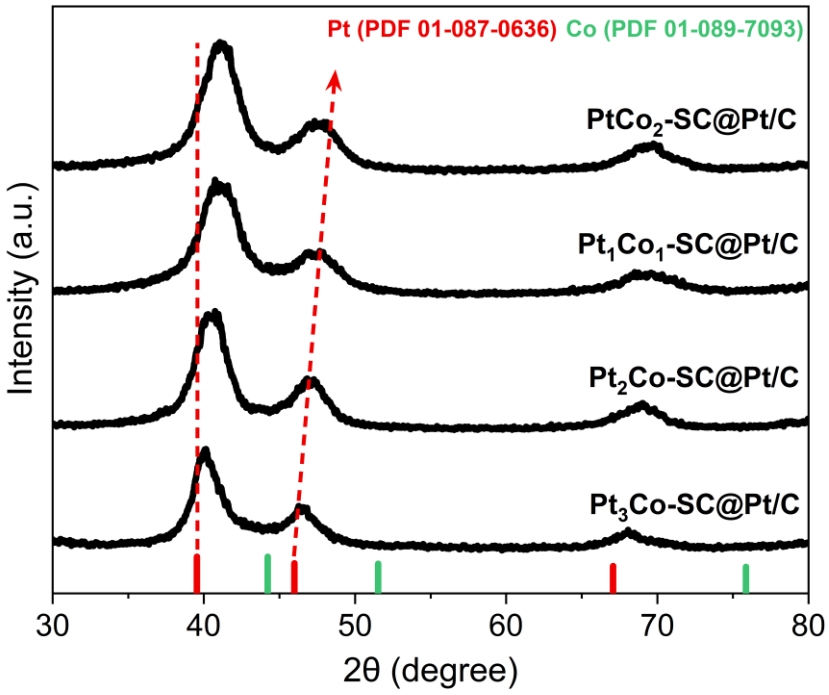


**Fig. S2.** XRD patterns of a catalyst series of PtCo-SC@Pt/C with different atomic compositions. The peaks are indexed by face-centered cubic (*fcc*) PtCo (PDF #03-065-8968).

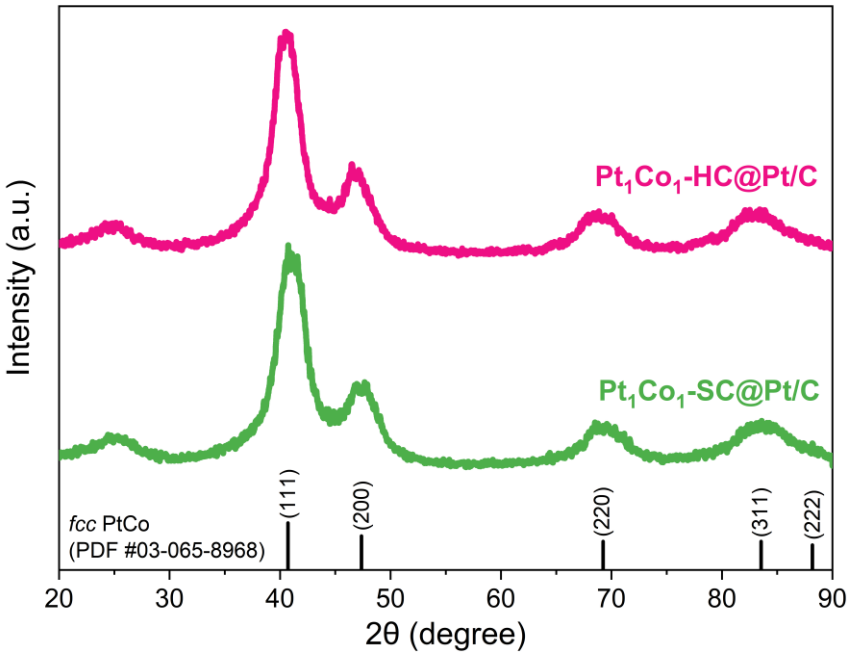


**Fig. S3.** XRD patterns of the obtained $Pt_1Co_1$-SC@Pt/C and $Pt_1Co_1$-HC@Pt/C catalysts. The peaks are indexed by face-centered cubic (*fcc*) PtCo (PDF #03-065-8968).

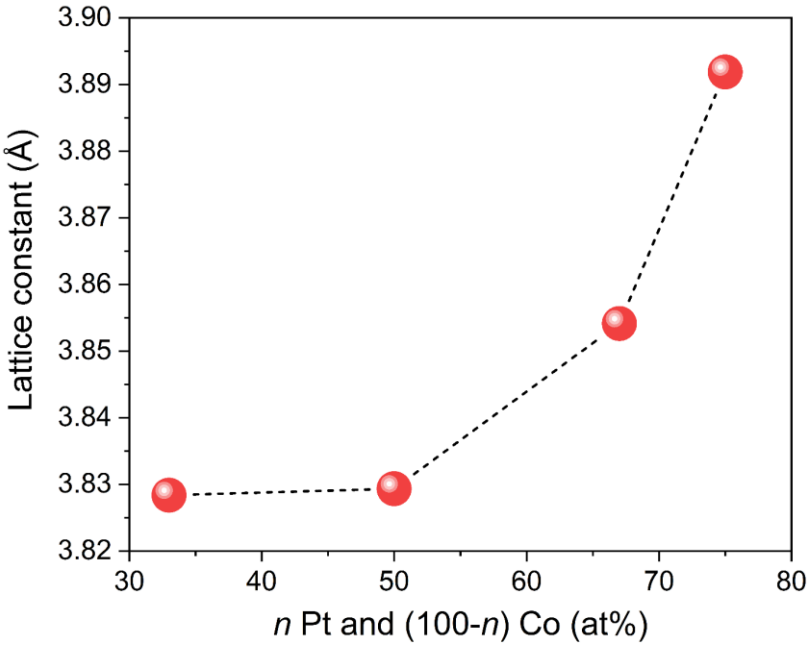


**Fig. S4.** Plot of Pt–Co compositions vs. lattice constant. Note that lattice constant was calculated based on Bragg's law.

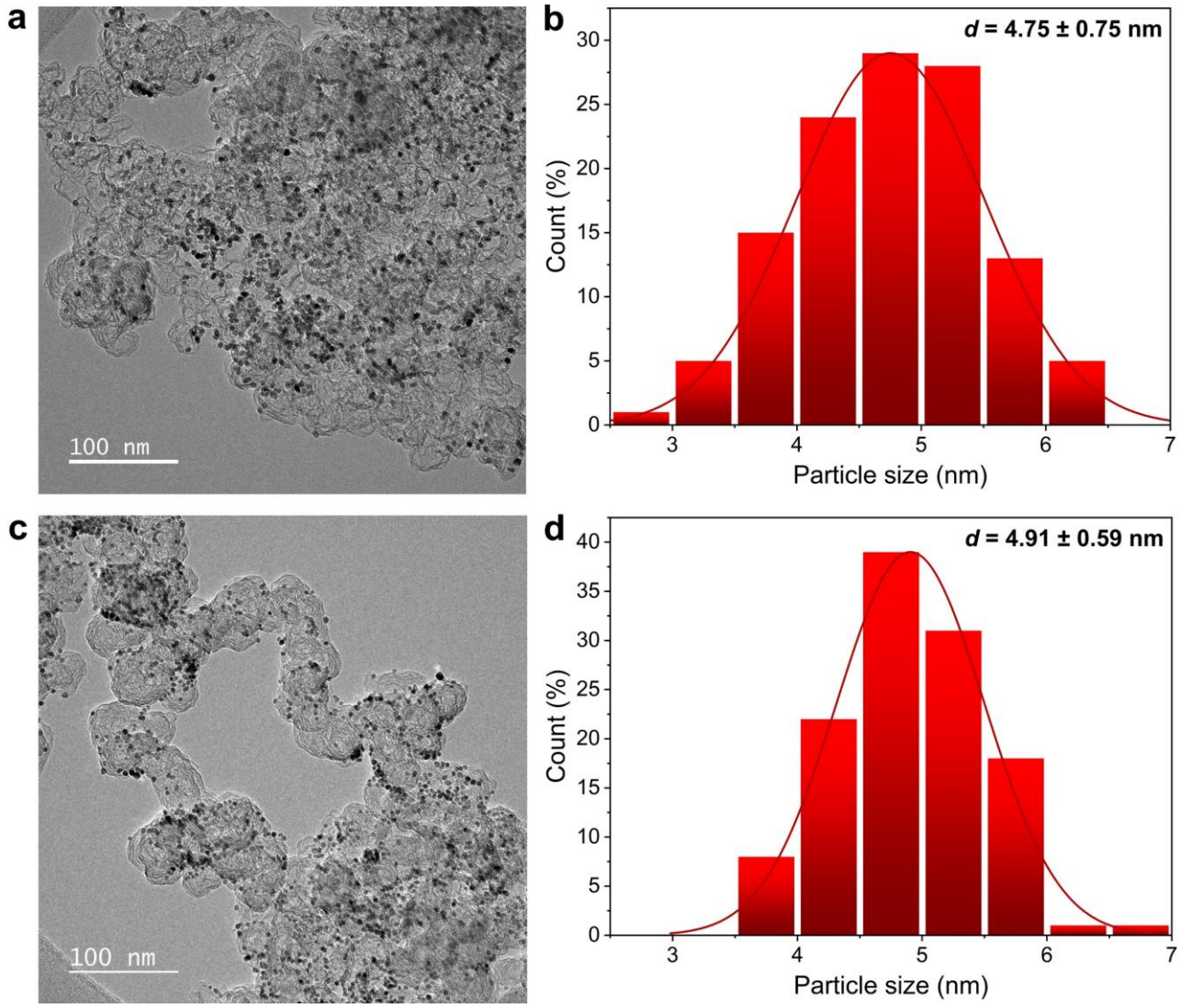


**Fig. S5.** (a, c) TEM images and (b, c) corresponding size distribution histogram of $Pt_1Co_1$-SC@Pt/C and $Pt_1Co_1$-HC@Pt/C catalysts, respectively.

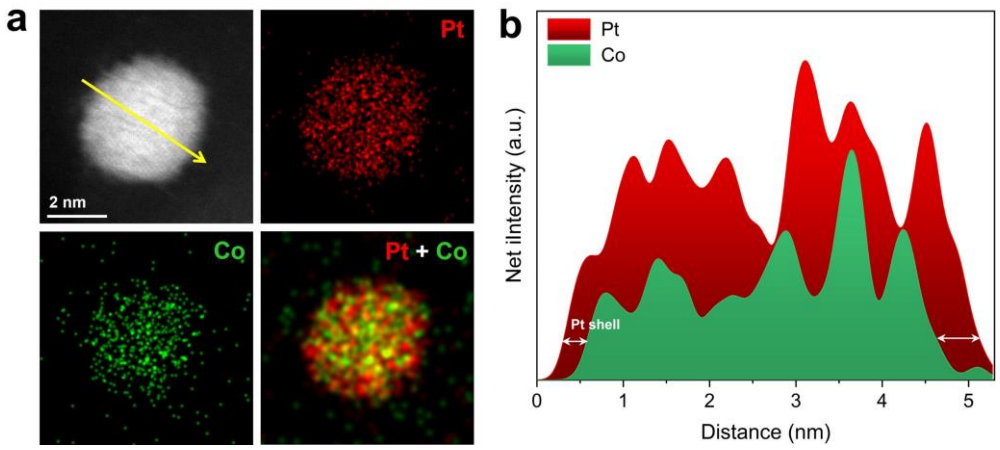


**Fig. S6.** (a) EDS elemental mapping images and (b) line scanning profiles for a single particle of $Pt_1Co_1$-SC@Pt/C.

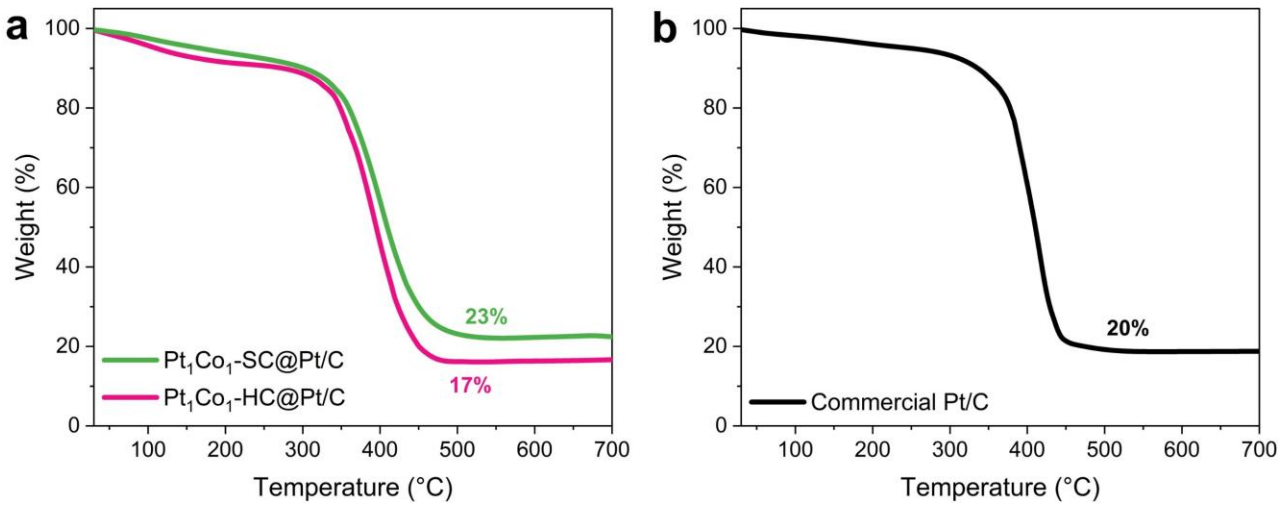


**Fig. S7.** TGA curves of (a) $Pt_1Co_1$-SC@Pt/C and $Pt_1Co_1$-HC@Pt/C catalysts and (b) commercial Pt/C in air condition.

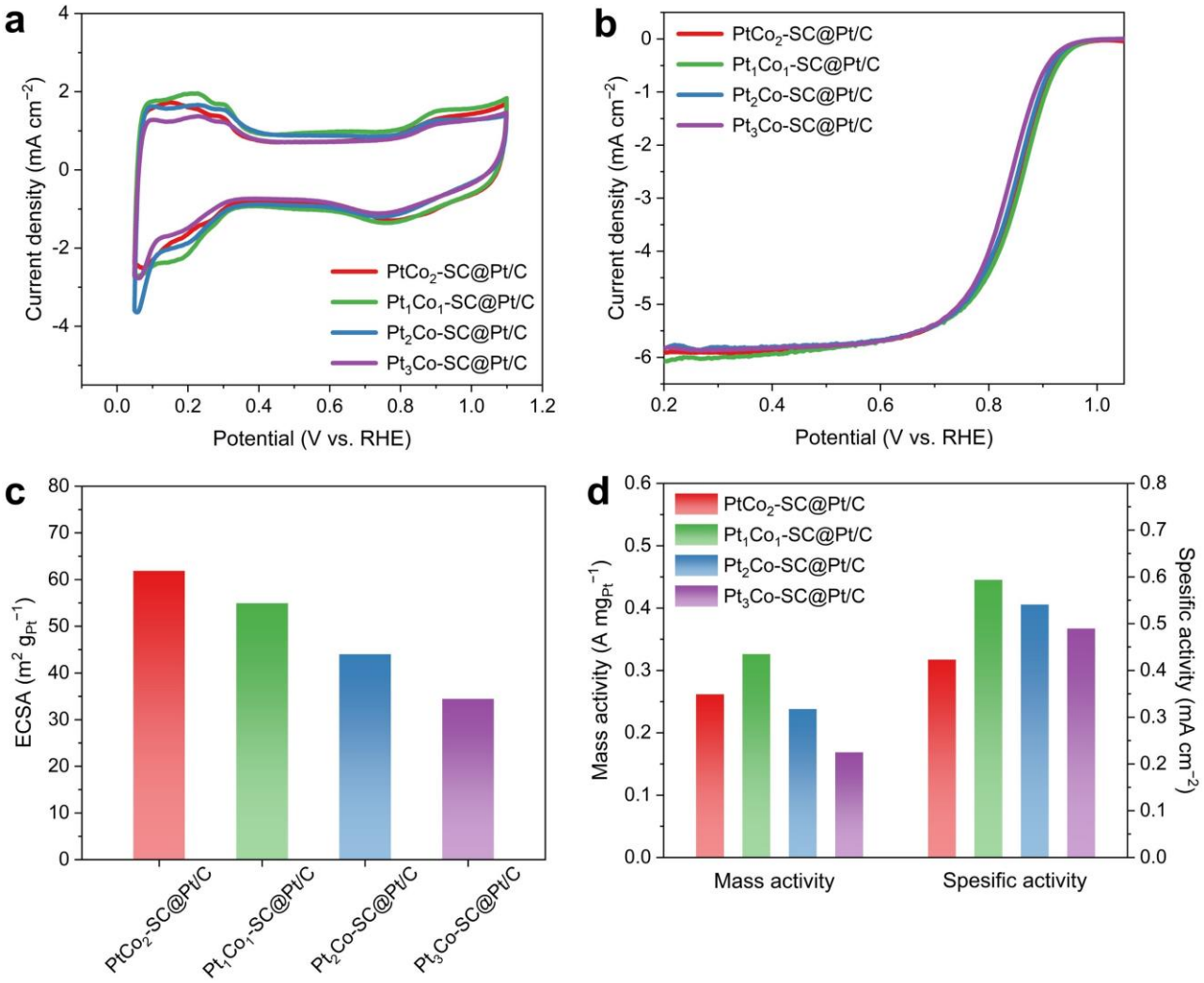


**Fig. S8.** (a) CVs, (b) LSVs, (c) ECSAs, and (d) mass and spesific activities of PtCo-SC@Pt/C catalyst libraries.

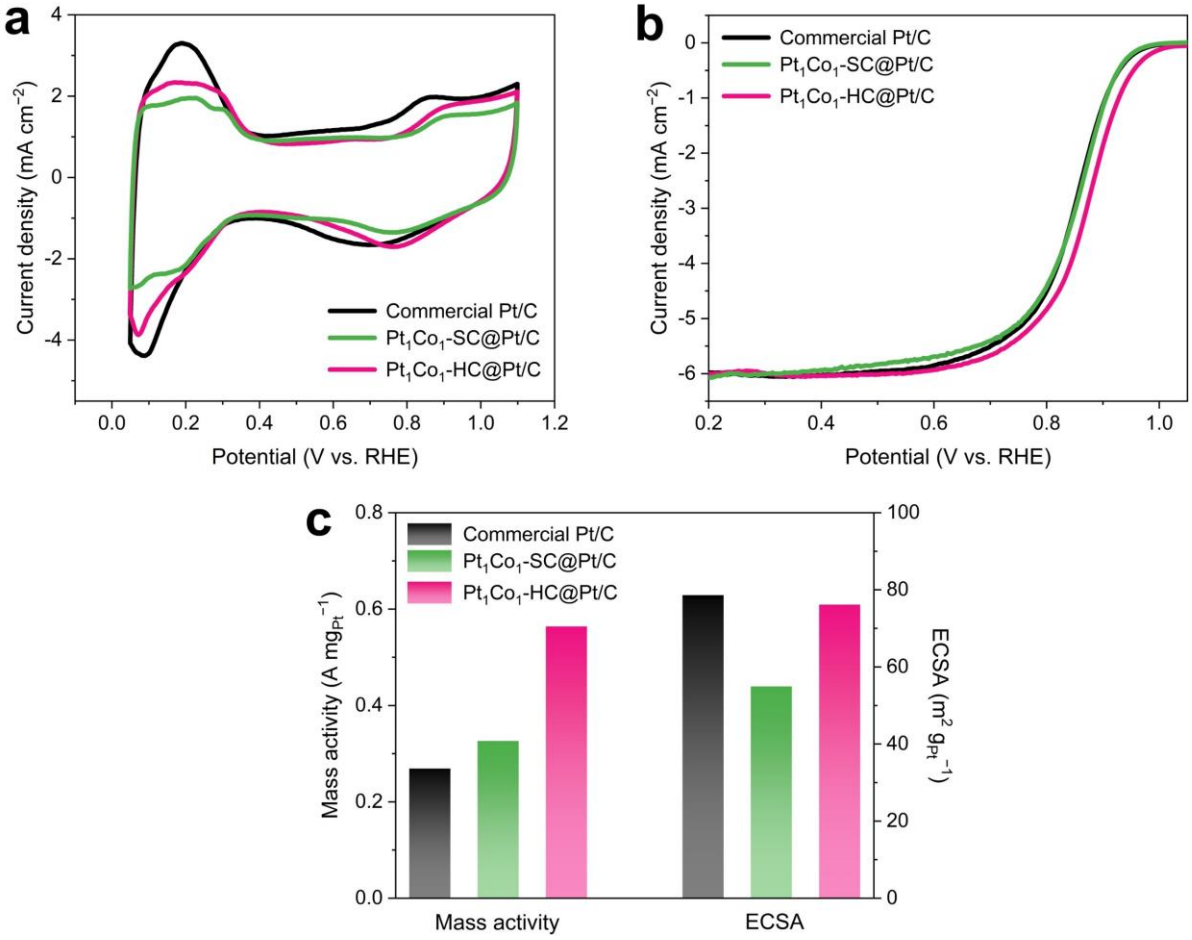


**Fig. S9.** (a) CVs, (b) LSVs, and (c) mass activities and ECSAs for commercial Pt/C, $Pt_1Co_1$-SC@Pt/C, and $Pt_1Co_1$-HC@Pt/C catalysts.

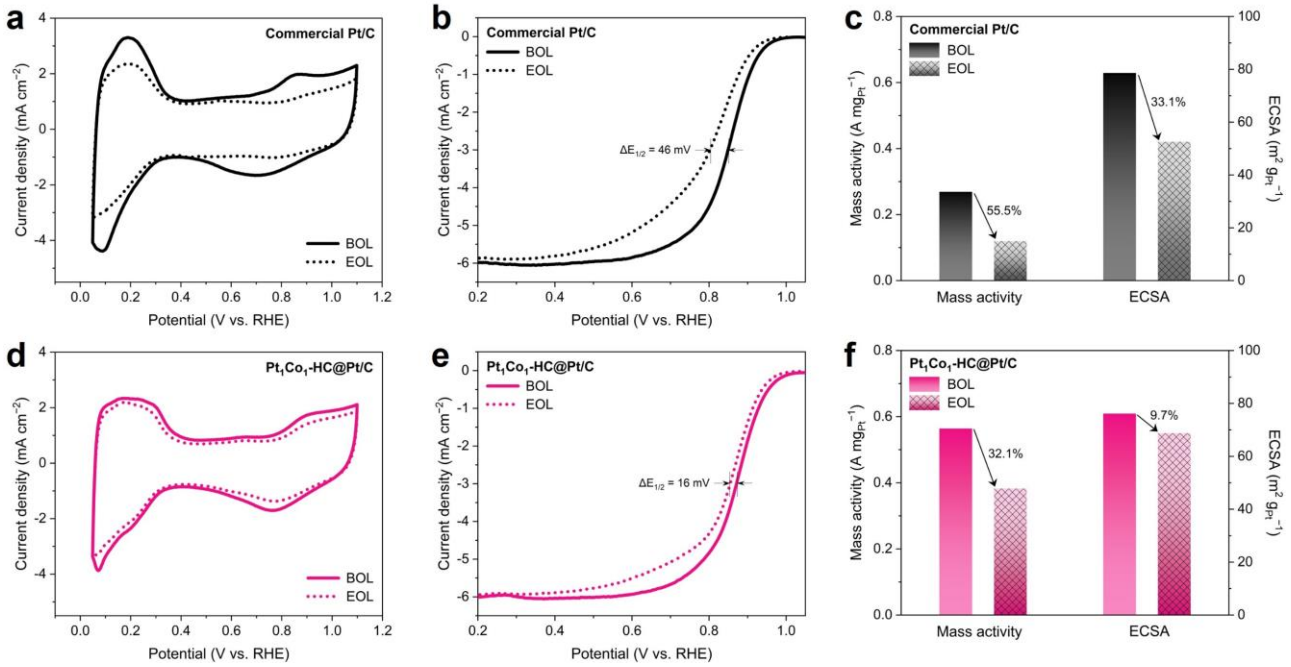


**Fig. S10.** (a, d) CVs, (b, e) LSVs, and (c, f) mass activities and ECSAs for commercial Pt/C and $Pt_1Co_1$-HC@Pt/C catalysts, respectively, before and after 30,000 cycles of AST.

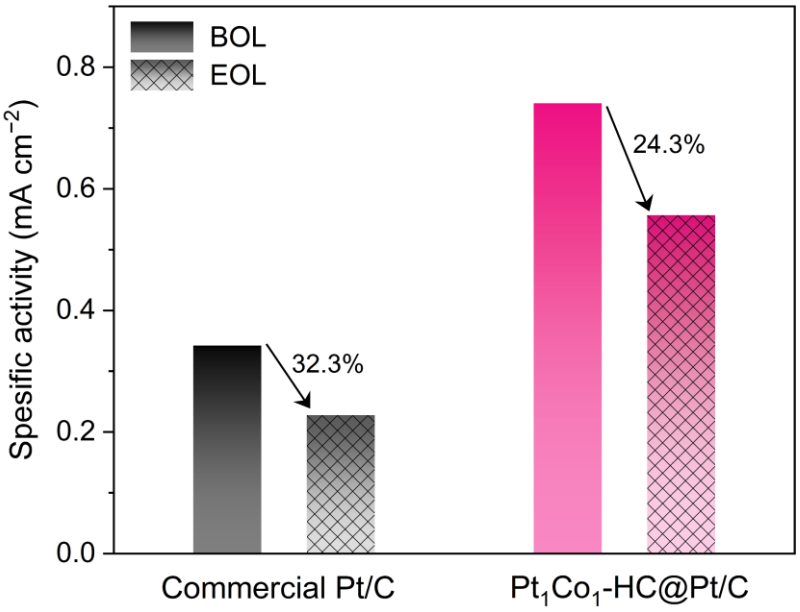


**Fig. S11.** Pt specific activity at 0.90 V for commercial Pt/C and $Pt_1Co_1$-HC@Pt/C before and after AST for 30,000 cycles.

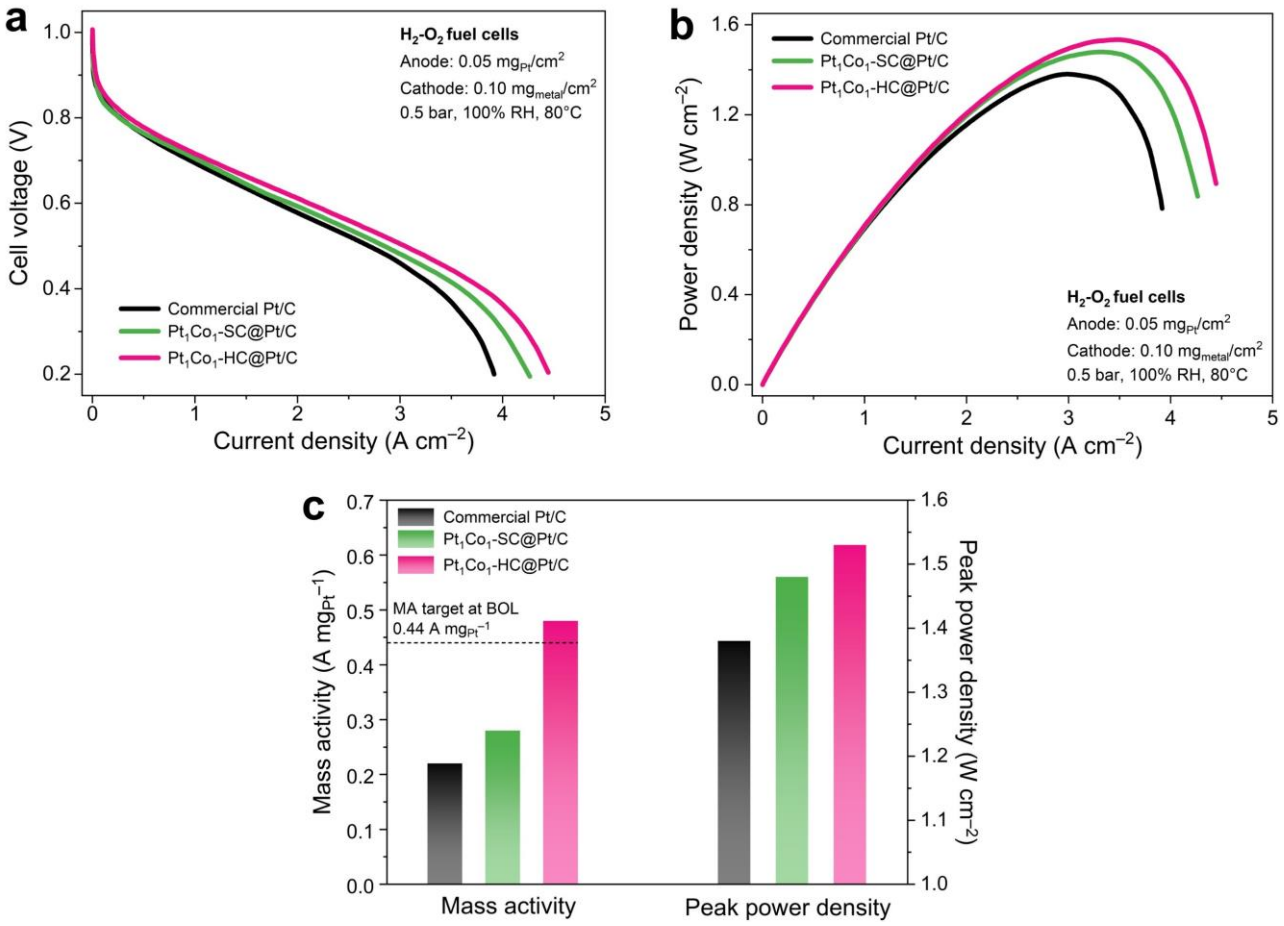


**Fig. S12.** (a) Polarization curves, (b) power density curves, and (c) corresponding mass activities at 0.9 V and peak power densities of MEAs with commercial Pt/C, $Pt_1Co_1$-SC@Pt/C, and $Pt_1Co_1$-HC@Pt/C as cathode catalysts under $H_2$–$O_2$ condition.

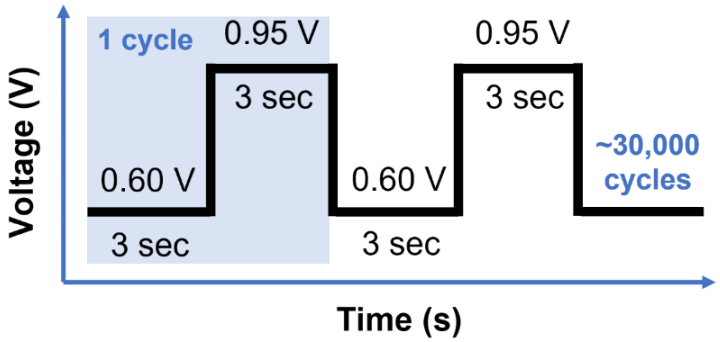


**Fig. S13.** US Department of Energy (DOE) AST protocols for electrocatalyst stability test.

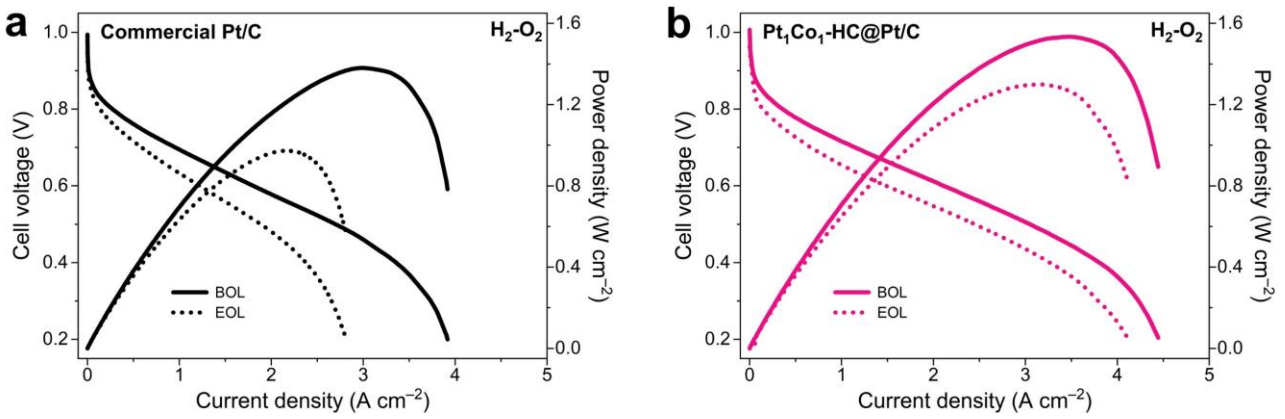


**Fig. S14.** $H_2$–$O_2$ polarization and power density curves of the MEAs fabricated by the cathode catalyst of (a) commercial Pt/C and (b) $Pt_1Co_1$-HC@Pt/C before and after 30,000 cycles of AST.

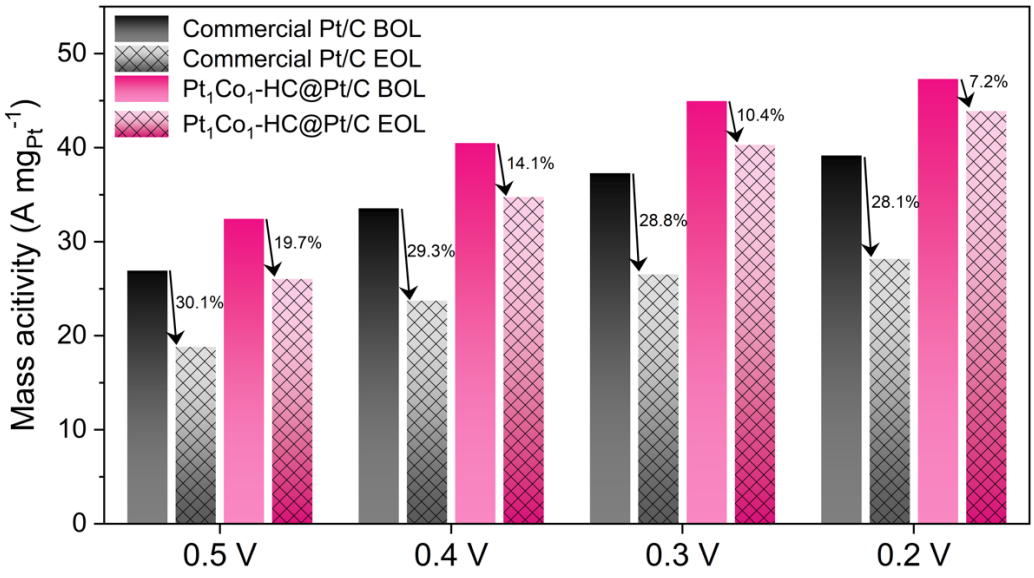


**Fig. S15.** MA degradation for commercial Pt/C and $Pt_1Co_1$-HC@Pt/C catalysts at various potentials before and after 30,000 AST cycles.

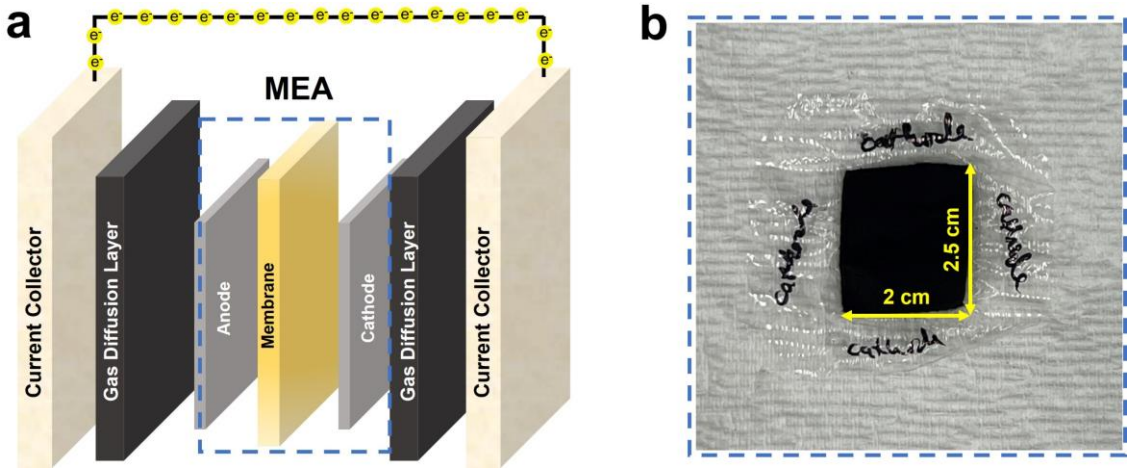


**Fig. S16.** (a) Schematic diagram of a single PEMFC. (b) Photograph of cathode part from top side view of the MEA.

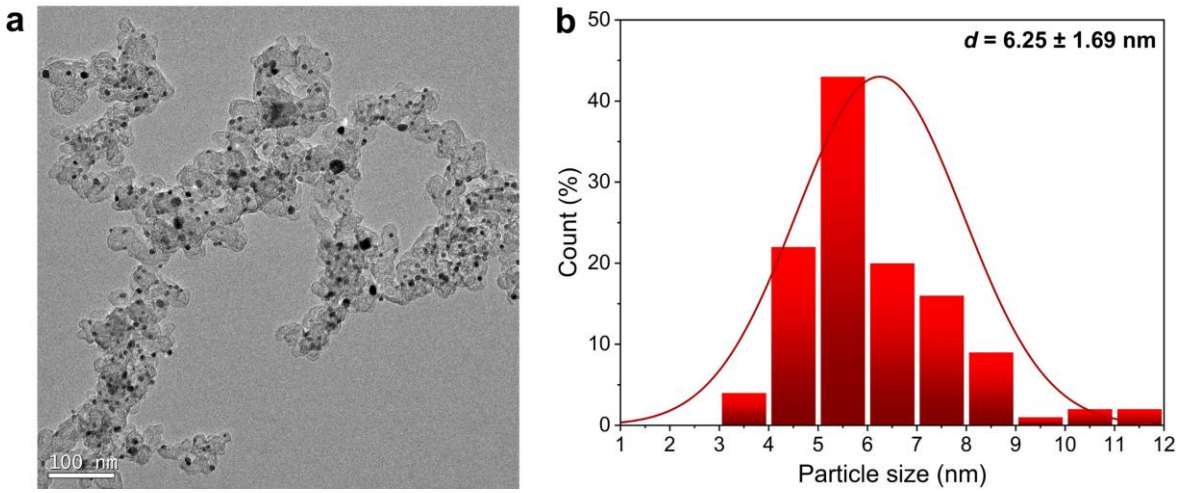


**Fig. S17.** (a) TEM image and (b) corresponding size distribution histogram of $Pt_1Co_1$-HC@Pt/C catalysts after 30,000 cycles of AST.

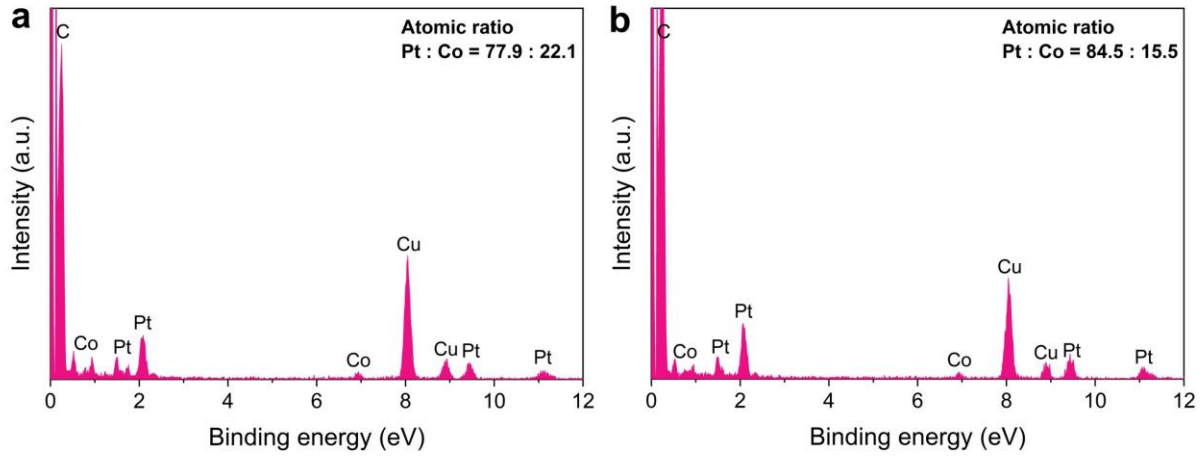


**Fig. S18.** EDS spectra of the MEAs of $Pt_1Co_1$-HC@Pt/C catalysts (a) before and (b) after 30,000 cycles of AST.

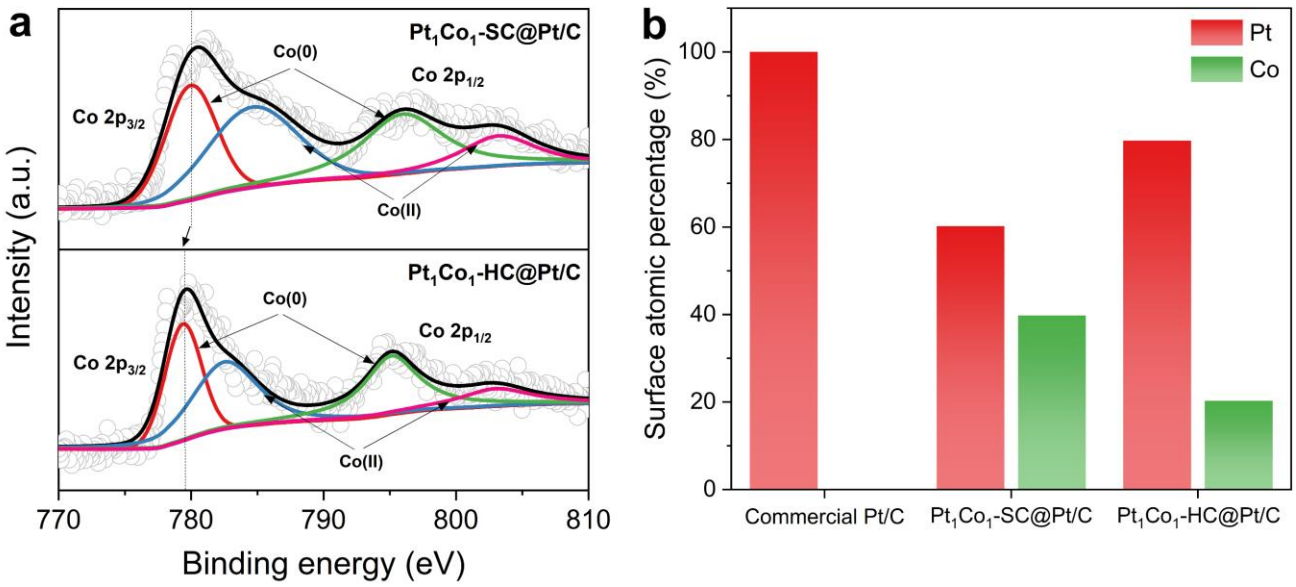


**Fig. S19.** (a) High-resolution XPS spectra of Co 2p for $Pt_1Co_1$-SC@Pt/C and $Pt_1Co_1$-HC@Pt/C catalysts. (b) Surface atomic composition of Pt and Co in commercial Pt/C, $Pt_1Co_1$-SC@Pt/C, and $Pt_1Co_1$-HC@Pt/C catalysts.

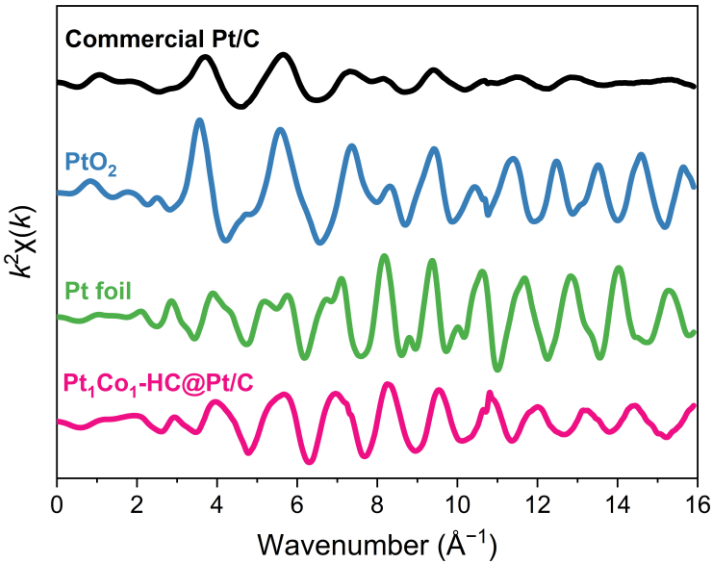


**Fig. S20.** EXAFS oscillations at Pt $L_3$-edge of commercial Pt/C, $PtO_2$, Pt foil, and $Pt_1Co_1$-HC@Pt/C catalysts.

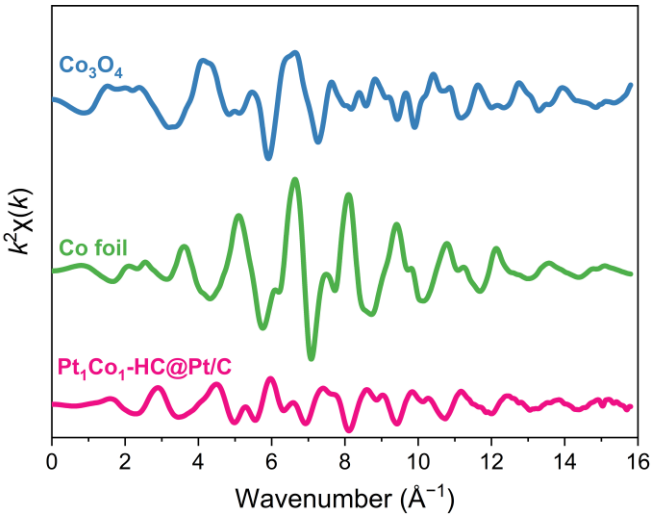


**Fig. S21.** EXAFS oscillations at Co K-edge of $Co_3O_4$, Co foil, and $Pt_1Co_1$-HC@Pt/C catalysts.

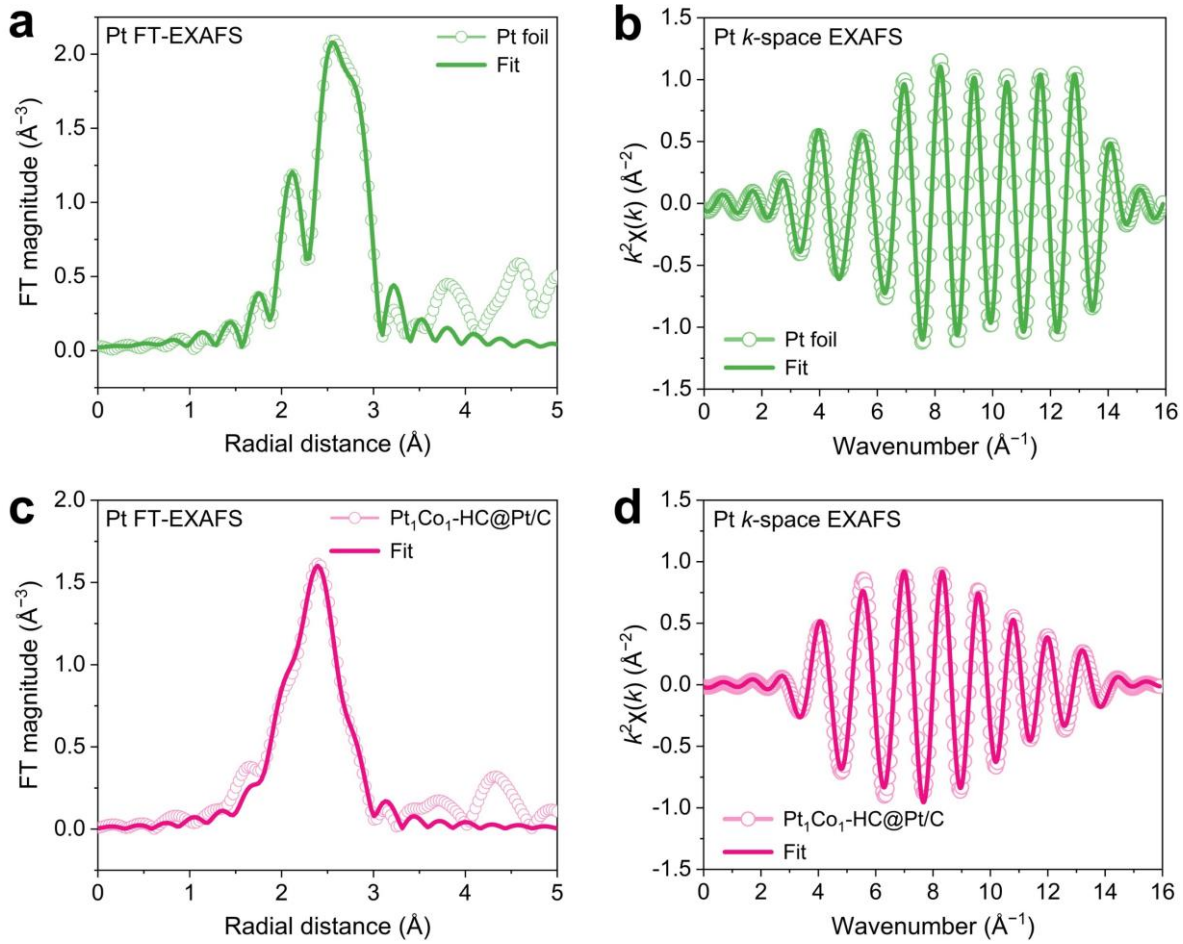


**Fig. S22.** (a, c) FT-EXAFS and (b, d) *k*-space EXAFS fitting results at Pt $L_3$-edge for Pt foil and $Pt_1Co_1$-HC@Pt/C, respectively.

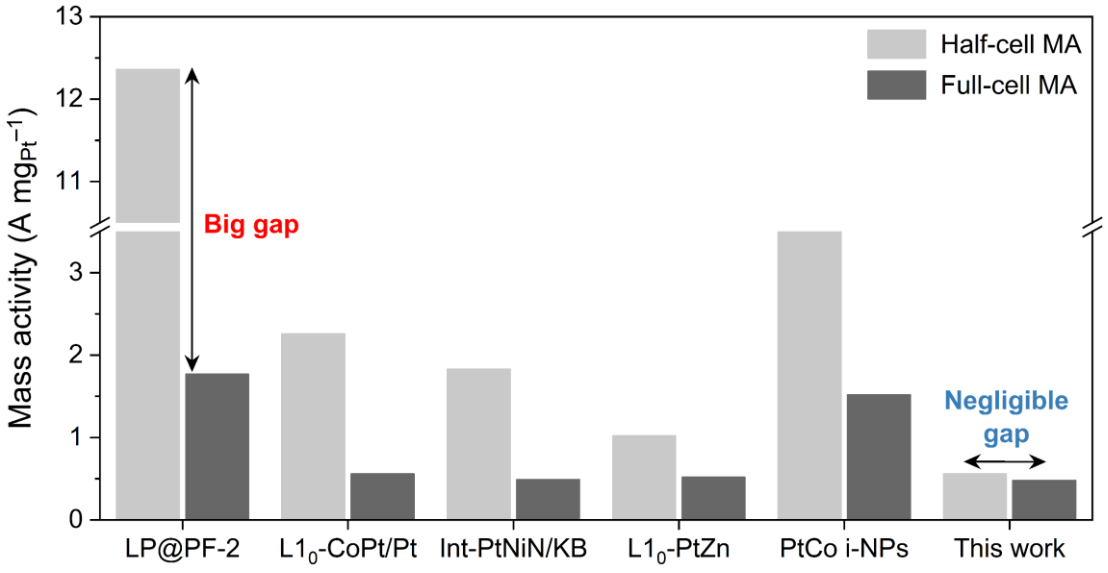


**Fig. S23.** The comparison of mass activity expression of state-of-the-art catalysts evaluated at RDE half-cell and MEA full-cell test, including LP@PF-2,[1] L1$_0$-CoPt/Pt,[2] Int-PtNiN/KB,[3] L1$_0$-PtZn,[4] and PtCo i-NPs.[5]

**Table S1.** Alloying degree of $Pt_1Co_1$-SC@Pt/C catalyst series according to Vegard's law and the (220) planes.

| Sample | 2θ (degree) | $a_{(220)}$ (Å) | χCo | [Co/Pt]* | Alloying degree** |
|---|---|---|---|---|---|
| $Pt_3Co$-SC@Pt/C | 68.09 | 3.892 | 0.098 | 0.25 | 43.4% |
| $Pt_2Co$-SC@Pt/C | 68.85 | 3.854 | 0.220 | 0.33 | 85.7% |
| $Pt_1Co_1$-SC@Pt/C | 69.35 | 3.829 | 0.301 | 0.50 | 86.1% |
| $PtCo_2$-SC@Pt/C | 69.47 | 3.823 | 0.320 | 0.67 | 70.1% |

*The [Co/Pt] is attained by the theoretical value of Co/Pt atomic ratio.

**The alloying degree is calculated by $\chi Co/(1 - \chi Co)[Co/Pt]$.

**Table S2.** Lattice constant and strain of Pt and PtCo NPs based on XRD results.

| | Crystal system | Lattice constant (Å) | Strain* (%) |
|---|---|---|---|
| | | ***a, b, c*** | ***a, b, c*** |
| Pt (PDF 01-087-0636) | Cubic | 3.944 | - |
| PtCo (PDF 03-065-8968) | Cubic | 3.850 | - |
| $Pt_1Co_1$-SC@Pt/C | Cubic | 3.829 | 2.92 |
| $Pt_1Co_1$-HC@Pt/C | Cubic | 3.852 | 2.33 |

*The contractions are calculated by $\varepsilon_a = (a_{Pt}–a)/a_{Pt}$, where $a_{Pt}$ is the lattice constant of Pt reference and $a$ represents the lattice constant $a$ in a unit cell.

**Table S3.** Composition of PtCo NPs electrocatalysts based on ICP-OES results.

| Catalyst | Weight ratio (Pt : Co) | Atomic ratio (Pt : Co) |
|---|---|---|
| $Pt_1Co_1$-SC@Pt/C | 81.8 : 18.2 | 57.5 : 42.5 |
| $Pt_1Co_1$-HC@Pt/C | 93.0 : 7.0 | 80.1 : 19.9 |

**Table S4.** ICP-OES results of the liquid 0.1 M $HClO_4$ electrolyte collected after half-cell ORR test of $PtCo_2$-SC@Pt/C and $Pt_1Co_1$-SC@Pt/C after the first 10,000 potential cycles.

| Electrolyte | Sample concentration (mg $L^{-1}$) | $[Pt]_{ICP}$ (mg $L^{-1}$) | $[Co]_{ICP}$ (mg $L^{-1}$) | Metal leaching* | |
|---|---|---|---|---|---|
| | | | | Pt | Co |
| Bare $HClO_4$ | 1.00 | NA | NA | NA | NA |
| $HClO_4$– $PtCo_2$-SC@Pt/C | 1.00 | 0.012 | 0.019 | 3.6% | 17.2% |
| $HClO_4$– $Pt_1Co_1$-SC@Pt/C | 1.00 | 0.014 | 0.008 | 3.9% | 9.9% |

*The metal leaching was calculated using the fraction of metal concentration in the aliquot determined with ICP-OES and the metal loading in the catalyst, $([M]_{ICP} \times V_{aliquot})/(m_{electrode} \times wt\%_{metal})$. $[M]_{ICP}$, $V_{aliquot}$, $m_{electrode}$, and $wt\%_{metal}$ denote the corresponding concentration of [Pt] or [Co] determined by ICP-OES, used volume of aliquot, mass of total metal loading on electrode, and weight percentage of the corresponding metal in the studied catalyst.

**Table S5.** Pt FT-EXAFS fitting results for Pt foil and $Pt_1Co_1$-HC@Pt/C.

| Sample | Path | CN* | *d** (Å) | $\sigma^2$* (Å) | R-factor* |
|---|---|---|---|---|---|
| Pt foil | Pt–Pt | 12.0 ± 0.4 | 2.764 ± 0.001 | 0.0047 ± 0.0001 | 0.002 |
| $Pt_1Co_1$-HC@Pt/C | Pt–Pt | 6.8 ± 1.5 | 2.696 ± 0.007 | 0.0059 ± 0.0010 | 0.001 |
| | Pt–Co | 1.5 ± 0.9 | 2.646 ± 0.011 | 0.0071 ± 0.0019 | |

*CN, coordination numbers; *d*, distance between absorber and backscatter atoms; $\sigma^2$, Debye-Waller factor; R-factor, a measure of the quality of the EXAFS fit.

## Reference


1 L. Chong, J. Wen, J. Kubal, F. G. Sen, J. Zou, J. Greeley, M. Chan, H. Barkholtz, W. Ding and D. J. Liu, *Science*, 2018, **362**, 1276–1281.

2 J. Li, S. Sharma, X. Liu, Y. T. Pan, J. S. Spendelow, M. Chi, Y. Jia, P. Zhang, D. A. Cullen, Z. Xi, H. Lin, Z. Yin, B. Shen, M. Muzzio, C. Yu, Y. S. Kim, A. A. Peterson, K. L. More, H. Zhu and S. Sun, *Joule*, 2019, **3**, 124–135.

3 X. Zhao, C. Xi, R. Zhang, L. Song, C. Wang, J. S. Spendelow, A. I. Frenkel, J. Yang, H. L. Xin and K. Sasaki, *ACS Catal.*, 2020, **10**, 10637–10645.

4 J. Liang, Z. Zhao, N. Li, X. Wang, S. Li, X. Liu, T. Wang, G. Lu, D. Wang, B. Hwang, Y. Huang, D. Su and Q. Li, *Adv. Energy Mater.*, 2020, **10**, 2000179.

5 C. L. Yang, L. N. Wang, P. Yin, J. Liu, M. X. Chen, Q. Q. Yan, Z. S. Wang, S. L. Xu, S. Q. Chu, C. Cui, H. Ju, J. Zhu, Y. Lin, J. Shui and H. W. Liang, *Science*, 2021, **374**, 459–464.